Inverse Scattering and Imaging in NDT: Recent Applications and Advances

René MARKLEIN, Jinghong MIAO, Mehbub-ur RAHMAN, Karl Jörg LANGENBERG,
University of Kassel, Department of Electrical Engineering and Computer Science,
Electromagnetic Field Theory, Kassel, Germany

Abstract. This overview paper presents recent advances and applications of different linear and nonlinear inversion algorithms in acoustics, electromagnetics, and elastodynamics. The inversion methods considered in this presentation vary from linear schemes, like the synthetic aperture focussing technique (SAFT) applied in ultrasonics and its counterpart in electromagnetics, the synthetic aperture radar (SAR), and the diffraction tomography (DT) or its implementation based on Fourier transforms (FT-SAFT), to nonlinear schemes, like the contrast source inversion (CSI) combined with different regularization approaches as well as the invariant embedding method, also known as the invariant embedding/layer stripping method. Inverse scattering and imaging results of the above mentioned inversion schemes are presented and compared for instance for ultrasonic and electromagnetic data from the Fraunhofer Institute for Nondestructive Testing (IZFP, Saarbrücken, Germany) and the Federal Research Institute for Material Research and Testing (BAM, Berlin, Germany).

Introduction

Latest advances and future challenges of the application of linear and nonlinear inversion schemes applied in nondestructive testing (NDT) are presented in the paper. Different inversion techniques are considered, which are applied in ultrasonic and electromagnetic NDT. These techniques comprise linear schemes, like the synthetic aperture focussing technique (SAFT), diffraction tomography (DT) or its implementation based on Fourier transforms (FT-SAFT), MUSIC algorithm, linear sampling method (LSM), and nonlinear schemes, like the modified gradient in field (MGF) method and the contrast source inversion (CSI) combined with different regularization approaches (see [1-6] and references therein). The 1-D profiling has become a point of interest in NDT, e.g., for material characterization and time-domain reflectometry (TDR) applications [7, 8]. In 1-D profiling the inverse problem is solved by invariant embedding/layer stripping [9, 10]. Results of the above mentioned schemes are presented and compared for measured ultrasonic and electromagnetic data.

1. Overview on the Applied Linear and Nonlinear Inversion Schemes

In this paper we apply different scalar inversion schemes to ultrasonic and electromagnetic data as listed below:

- Synthetic aperture focusing technique (SAFT): SAFT in ultrasonics is a linear phenomenological imaging technique [1-3]. This technique is based on the heuristic interpretation of the time-domain 3-D Green's function of free-space

$$G(\underline{\mathbf{R}}-\underline{\mathbf{R}}',t)=\frac{1}{4\pi\,|\,\underline{\mathbf{R}}-\underline{\mathbf{R}}'\,|}\,\delta\left(t-\frac{|\underline{\mathbf{R}}-\underline{\mathbf{R}}'|}{c_0}\right) \tag{1}$$

and the relating diffraction surface of a point scatterer in the *xyt* data set (see Fig. 1).

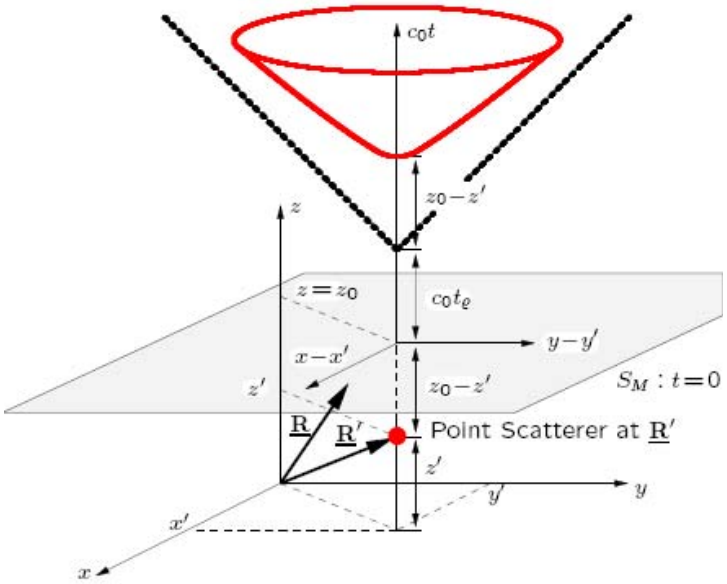

Figure 1: Diffraction surface (red) of a point scatterer (red dot)

- Diffraction tomography (DT): the applied linear scalar DT algorithm solves the linearized Porter–Bojarski integral equation using the first-order Born approximation utilizing the K-space calculus. Details of the algorithm can be found e. g. in [1-3].
- TR/MUSIC algorithm: the time-reversal multiple signal classification (MUSIC) method from sub-space signal processing was first applied in inverse scattering in [11]. Thus, the MUSIC applied in inverse scattering requires is based on the multi-static data, the multi-static response (MSR) matrix, the time–reversal (TR) matrix as well as on the eigenvalues and eigenvectors of the TR matrix.
- Linear sampling method (LSM): there are different versions of LSM, which uses a factorization method applied to the far-field operator for shape reconstruction of the scatterer. We apply the LSM version using Tikhonov regularization where the regularization parameter is chosen by the Morozov's generalized discrepancy principle (see [5, 6] and references therein).
- Modified gradient in field (MGF) method: in the MGF method the inverse problem is posed as an optimization problem where a scalar cost functional is minimized [9]. The unknowns are the total field and the contrast function and the updates of the unknowns are computed simultaneously at each iteration step using two CG methods running concurrently. MGF is designed for dielectric targets, while for metallic (conducting) targets a modified scheme called MGFM is applied (see [3, 4] and references therein).
- Contrast source inversion (CSI): this method is like the MGF method an iterative algorithm, where the unknown field quantities are the contrast source and the material contrast. Here, the contrast source is the product of the material contrast and the total field. A variant is CSIW derived by using weighted contrast sources where the contrast source and the total field are weighted by the incident field. It has been observed that the CSIW performs better than the CSI (see [3, 4] and references therein).

- Extended CSI (ECSI): the ECSI works in a similar way as the CSI, except that the contrast is updated using a conjugate gradient iteration at every step instead of the analytical method used in CSI. Additionally, the ECSI uses a total variation (TV) based regularization (see [3, 4] and references therein).
- Invariant embedding/layer stripping method: this technique is based on a wave splitting approach and takes the reflected and transmitted wave field to determine the material properties of the medium, permittivity and electric conductivity by an embedding equation [9, 10].

2. Linear and Nonlinear Inversion of Electromagnetic Remote Sensing Data

At first we recall some results obtained for electromagnetic remote sensing data. The achieved results stimulated the application of these nonlinear schemes to ultrasonic data. Fig. 2a shows a perfectly electrically conducting (PEC) rectangular metallic cylinder, which is one of the targets of the Fresnel data set measured at the Institut Fresnel, Marseille, France. The experimental setup is described in [3, 5] and references therein. Results of DT, MUSIC/TR, K–LSM–TI, CSIW, and ECSI are given in Fig. 2b–2f. The DT and MUSIC/TR results are comparable, while the K–LSM–TI is better than the DT and MUSIC results. The image obtained with ECSI seems to be bigger in comparison with the actual dimensions or with the other reconstructions, but the position and shape have been properly reconstructed; it gives the best results, which stimulated the application of these nonlinear inversion approaches in ultrasonic NDT.

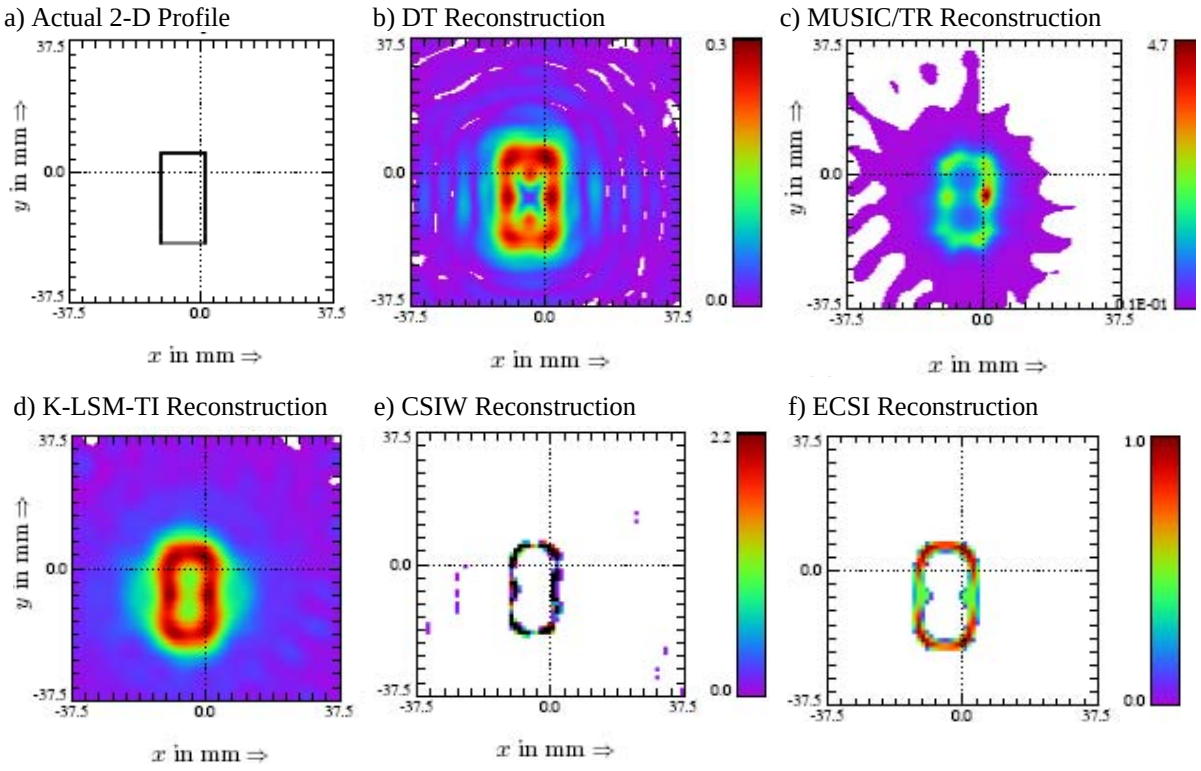

Figure 2: Reconstruction results for a centred metallic rectangular cylinder (PEC) target of electromagnetic Fresnel data with TM polarization: a) Actual shape and position, b) DT reconstruction, c) MUSIC reconstruction, d) K–LSM–TI reconstruction, e) CSIW reconstruction, f) ECSI reconstruction The results in b)-d) are obtained using the 16 GHz data. The results in e) and f) are achieved using the frequency-hopping approach with the data at 4, 8, 12 and 16 GHz.

3. Linear and Nonlinear Inversion of Ultrasonic and Electromagnetic NDT Data

Fig. 3 shows the geometries and photographs of four aluminium samples with two, four, six, and twelve air-filled circular cylinders which are in the experiments embedded in a water tank. Multi-pulse-echo and multi-pitch-catch ultrasonic data sets have been carefully measured (see Fig. 6b). A SAFT reconstruction of the multi-pulse-echo data is given in Fig. 4 and of the multi-pitch-catch data is given in Fig. 5. Nonlinear CSI inversion results presented in Fig. 6d)-f) are in general sharper and has less artefacts than the SAFT results. Even an extension of SAFT to the inhomogeneous anisotropic case, which yields the InASAFT, is working well and in combination with numerical modelling tools, like EFIT [2, 12, 13], the effects of linearization, for instance artefacts in the reconstruction, can be interpreted [12, 13]. Obviously, like in the ultrasonic case, simulated electromagnetic data imaging using SAFT and its frequency-domain counterpart called Fourier transform-SAFT (FT-SAFT) lead to an intuitive physical understanding of GPR probing of embedded structures in concrete [14].

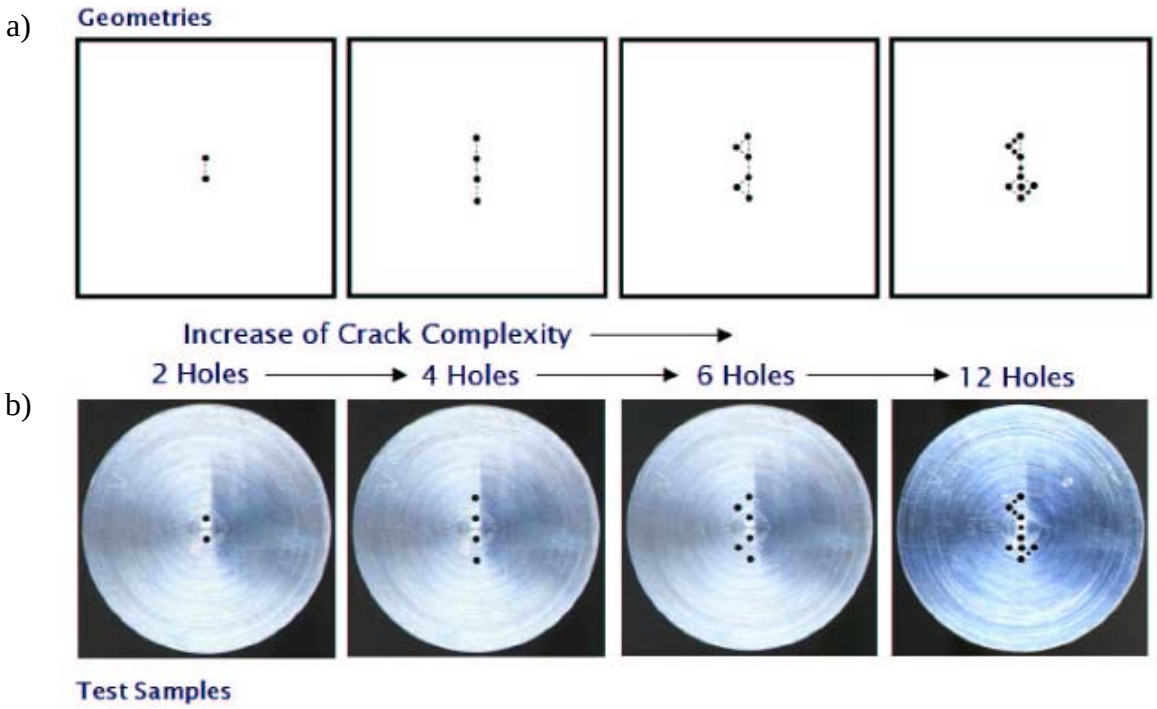

Figure 3: The stepwise increase of crack complexity: a) samples geometries of two, four, six and twelve holes, b) aluminium samples

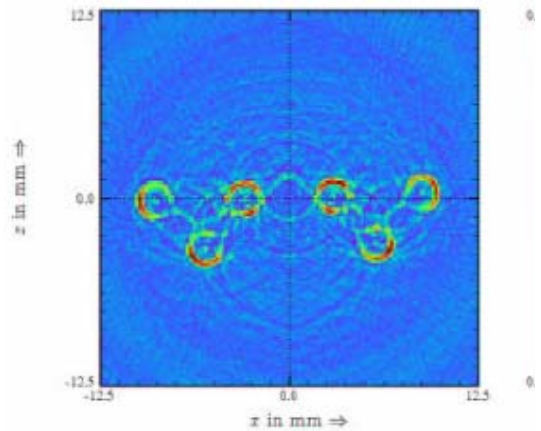

Figure 4: SAFT reconstruction of the multi-pulse-echo data set

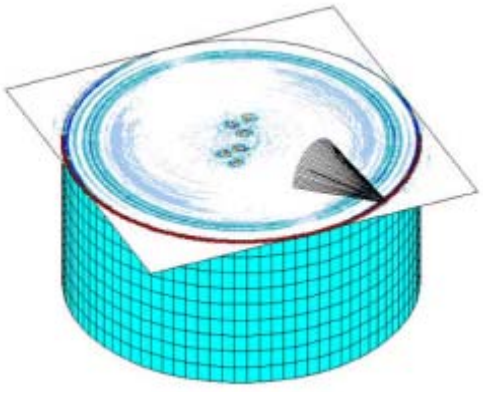

Figure 5: SAFT reconstruction embedded in the 3-D geometry of the test sample

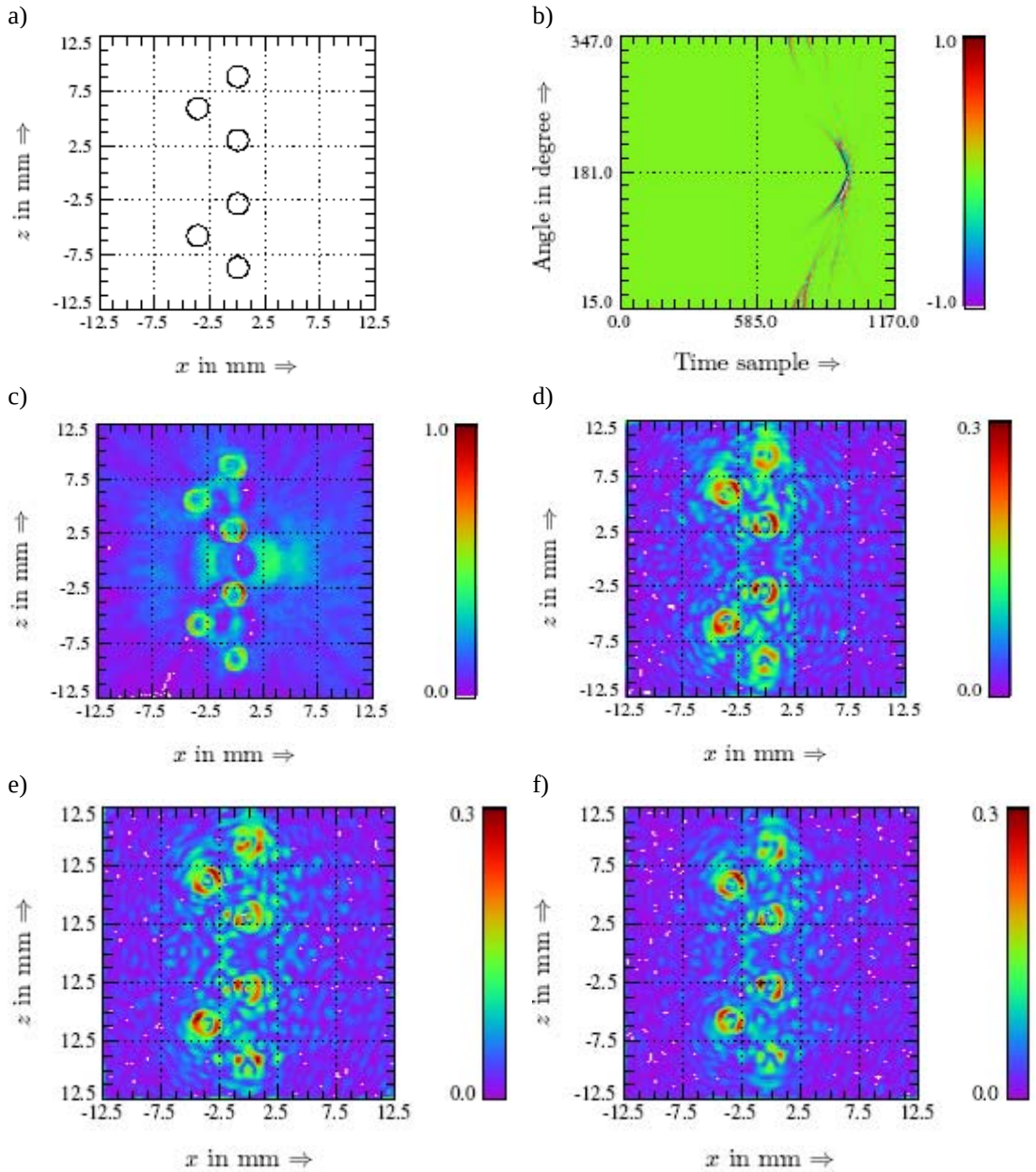

Figure 6: Linear and nonlinear inversion results: a) actual profile, b) measured ultrasonic multi-pitch-catch time-domain data set for the transmitter at 0°, c) time-domain SAFT reconstruction, d) frequency-domain CSI reconstruction using data at six different frequencies, no *a priori* information used, e) frequency-domain CSI reconstruction using single frequency data and *a priori* information, the contrast is imaginary valued, f) frequency-domain CSI reconstruction using data at four different frequencies and *a priori* information, the contrast is imaginary valued

4. 1-D Profiling in NDT and Material Characterization

A typical 1-D profiling situation is given in Fig. 7, where a nonmagnetic 1-D slab with an inhomogeneous permittivity and electric conductivity profile is considered. Based on the wave equation synthetic data are computed as a testbed for the applied time-domain inversion schemes. The inverse scattering algorithm is based on the invariant embedding/layer stripping approach [9, 10]. The input to this algorithm for 1-D profiling is the reflection and transmission kernel to reconstruct the permittivity and electric conductivity profile. Therefore, a deconvolution of the reflected and transmitted data as well as the incident field must be performed. In the following three examples are presented.

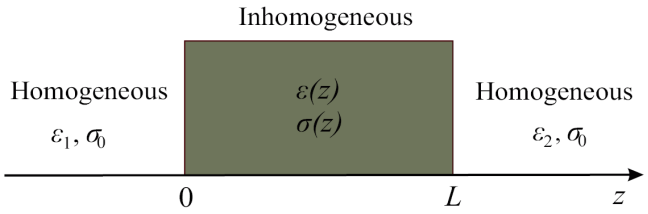

Figure 7: Geometry of the inhomogeneous slab

4.1 Example 1. In the first example the relative permittivity profile of a sinusoidal shaped slab is reconstructed with an incident delta-pulse. The reconstructed relative permittivity profile is shown in Fig. 8, which coincides with the original profile even for this smooth profile where no prominent interfaces are present.

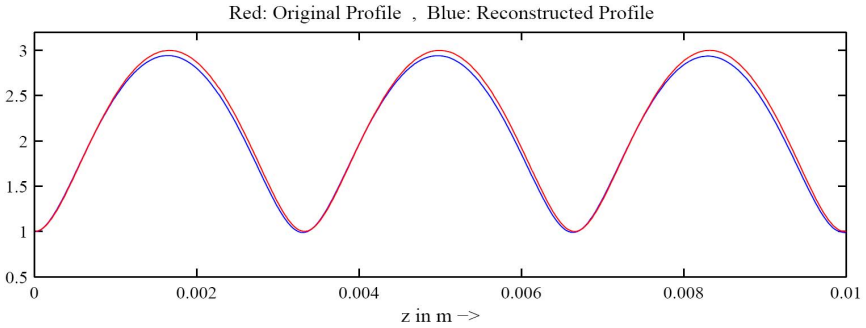

Figure 8: Original relative permittivity profile of the slab (red) and reconstructed profile (blue)

4.2 Example 2. In this example a sinusoidal wave of a frequency of 2.45 GHz is chosen. The incident wave is impinged from the top side at the centre of the multi-layered geometry given in Fig. 9. The incident wave and the synthetic reflected wave from the slab computed with a forward solver are drawn in Fig. 10. The reconstructed relative permittivity and conductivity profile are given in Fig. 11 and Fig. 12, respectively. Both reconstructed profiles follow closely to the original profile. Discrepancies between the original and reconstructed profiles occur towards the end of the slab due to multiple reflections from the boundaries of the layers.

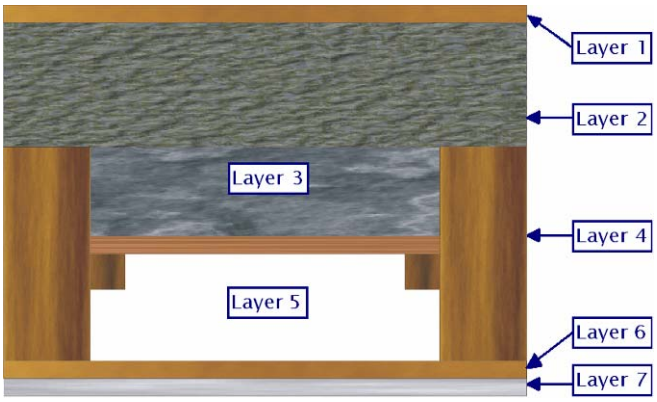

Figure 9: Geometry of the multi-layered test slab

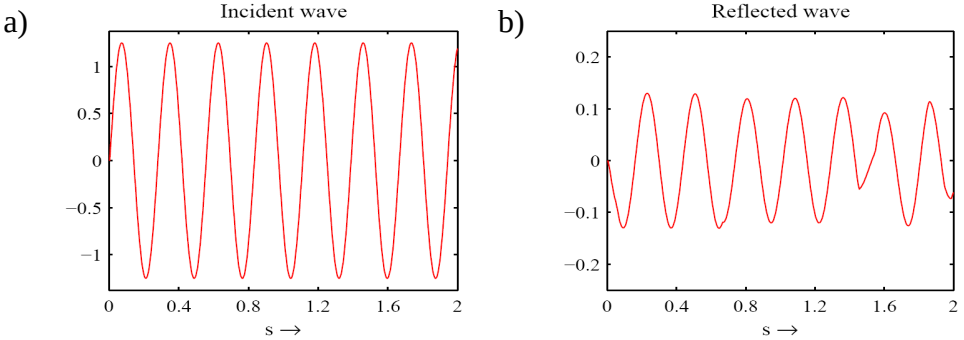

Figure 10: a) Incident wave (left) and reflected wave (right)

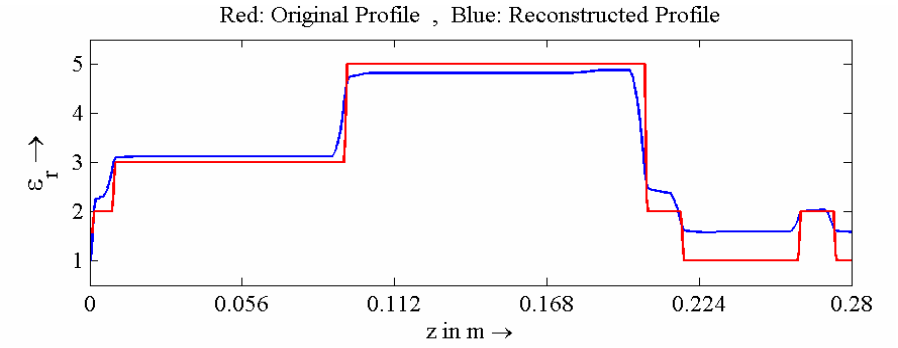

Figure 11: Original relative permittivity profile of the slab (red) and reconstructed profile (blue)

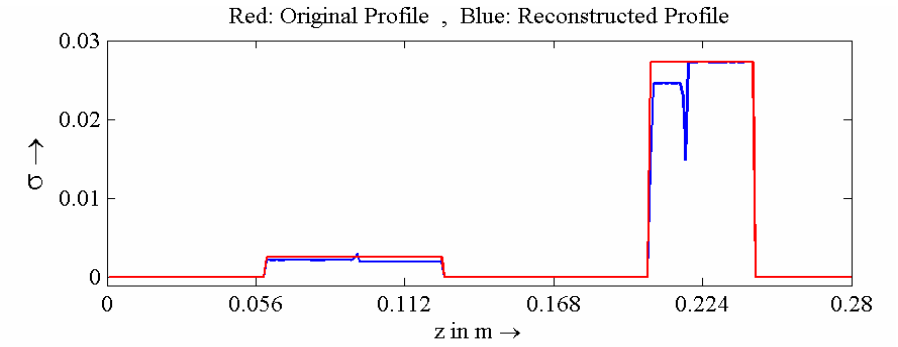

Figure 12: Original conductivity profile of the slab (red) and reconstructed profile (blue)

4.3 Example 3. In the third example measured reflection data, provided by the BAM, Berlin, Germany, have been processed. The excitation signal is a step function as given in Fig. 13a which is typically applied in time-domain reflectometry (TDR) and the measured A-scan is given in Fig. 13b. The slab is made of lime sandstone, which has a relative permittivity in the range of 5-8 depending on the moisture content and the amount of impurities inside. The inversion results presented in Fig. 13c have been validated by computing synthetic reflection data of the reconstructed profile. Both data sets coincided.

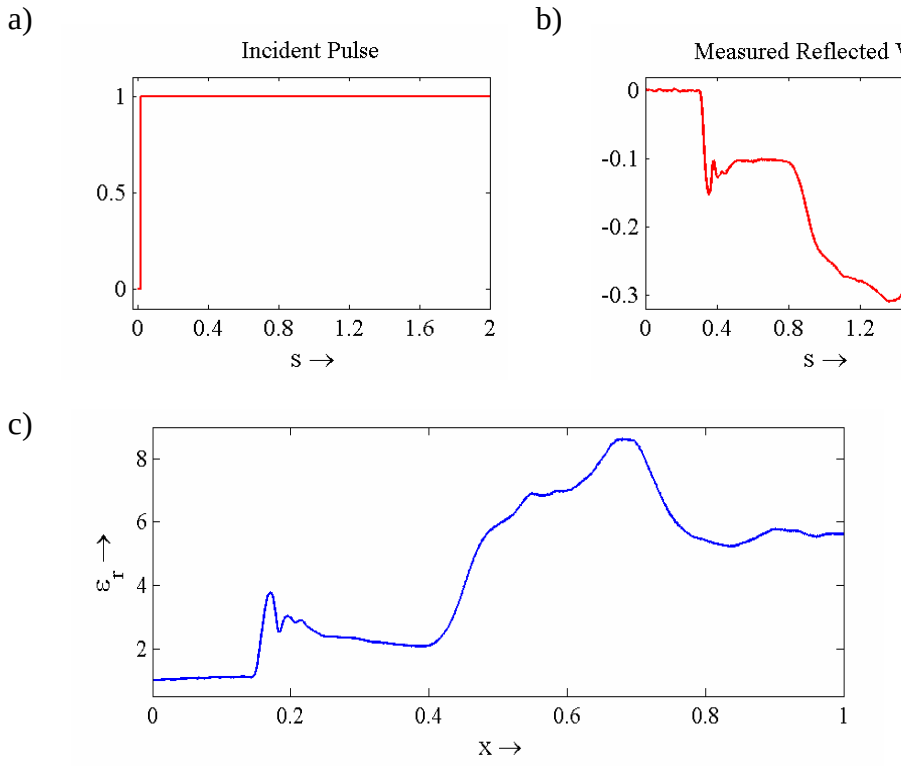

Figure 13: a) incident wave, b) reflected wave, A-scan, from a lime sandstone slab, c) reconstructed profile of the lime sandstone

Conclusions

We have presented results of various linear and nonlinear inversion applied to ultrasonic and electromagnetic data. These results demonstrate the considerable potential to extend and improve the ultrasonic imaging technique SAFT. The 1-D profiling results have been presented for synthetic and measured data. Presently we are working on several improvements, e.g., the polarimetric inversion schemes for NDT and the application of the 1-D profiling algorithms for moisture characterization in NDT-CE.

Acknowledgement

We gratefully thank Dr. V. Schmitz (retired) for the measured ultrasonic data reconstructed in Sec. 3 and Dr. Ch. Sklarczyk who stimulated the application given in Sec. 4.2, both are from the IZFP, Saarbrücken, Germany, as well as we gratefully thank Dr. Ch. Maierhofer from the BAM, Berlin, Germany for the provided TDR data reconstructed in Sec. 4.3.

References

[1] Langenberg, K. J., 2002, Linear Scalar Inverse Scattering, Vol. 1, pp. 121-141. in Pike, E. R., Sabatier, P. C. (eds.), *Scattering: Scattering and Inverse Scattering in Pure and Applied Science*, Academic Press, London.

[2] Langenberg, K. J., Marklein, R., Mayer, K., 2002, Applications to Nondestructive Testing with Ultrasound, Vol. 1, pp. 594-617, in Pike, E. R., Sabatier, P. C. (eds.), *Scattering: Scattering and Inverse Scattering in Pure and Applied Science*, Academic Press, London.

[3] Marklein, R., K. Mayer, R. Hannemann, T. Krylow, K. Balasubramanian, K. J. Langenberg, and V. Schmitz, 2002, Linear and nonlinear inversion algorithms applied in nondestructive evaluation, *Inverse Problems*, Vol. 18, No. 6, pp. 1733-1759.

[4] van den Berg, P. M., 2002, Nonlinear Scalar Inverse Scattering: Algorithms and Applications, Vol. 1, pp. 142-161, in Pike, E. R., Sabatier, P. C. (eds.), *Scattering: Scattering and Inverse Scattering in Pure and Applied Science*, Academic Press, London.

[5] Marklein, R., Balasubramanian, K., Langenberg, K. J., Miao, J., Sinaga, S. M., 2002, Applied Linear and Nonlinear Scalar Inverse Scattering: A Comparative Study, in *Proc. XXVIIth General Assembly of the International URSI*, http://ursiweb.intec.ugent.be/Proceedings/ProcGA02/papers/p1694.pdf.

[6] Potthast, R., 2006, A Survey on Sampling and Probe Methods for Inverse Problems, *Inverse Problems*, Vol. 22, pp. R1-R47.

[7] Connor, K. M., Dowding, C. H., 1999, *GeoMeasurements by Pulsing TDR Cables and Probes*, CRC Press, Boca Raton, USA.

[8] Dowding, Ch. H. (ed.), 2001, *Proceedings of the Second International Symposium and Workshop of Time Domain Reflectometry for Innovative Geotechnical Applications*, Infrastructure Technology Institute, Evanston, IL, USA, www.iti.northwestern.edu/tdr/tdr2001/proceedings/Final/TDR2001.pdf.

[9] Kristensson, G., Krueger, R. J., 1986, Direct and inverse scattering in the time domain for a dissipative wave equation. Part 1 and 2, *Journal of Mathematical Physics*, Vol. 27, No. 6, pp. 1667-1693.

[10] Fuks, P., Kristensson, G., Larson, G., 1990, *Permittivity Profile Reconstructions Using Transient Electromagnetic Reflection Data*, Report, Dept. Electroscience, Electromagnetic Theory, Lund Institute of Technology, Sweden, http://www.es.lth.se/teorel/Publications/TEAT-7000-series/TEAT-7009.pdf

[11] Devaney, A. J., 2000, Super-resolution processing of multi-static data using time reversal and MUSIC, Department of Electrical and Computer Engineering., Northeastern University, Boston, USA, *www.ece.neu.edu/faculty/devaney*.

[12] Shlivinski, A., Langenberg, K. J., Marklein, R., 2004, Ultrasonic Modelling and Imaging in Dissimilar Welds", in *Proc. 30th MPA-Seminar/ 9th German-Japanese Seminar*, Stuttgart, Germany.

[13] Shlivinski, A., Langenberg, K. J., Marklein, R., Schmitz, V., Müller, W., Mletzko, U., 2004, Modelling of Elastic Wave Propagation and Imaging of Defects in Dissimilar Welds, in *Proc. 4th International Conf. on NDE in Relation to Structural Integrity for Nuclear and Pressurised Components*, London, UK.

[14] Langenberg, K.-J., Mayer, K., Marklein, R., 2006, Nondestructive Testing of Concrete with Electromagnetic and Elastic Waves: Modeling and Imaging, *Cement & Concrete Composites*, Vol. 28, pp. 370-383.